ON SURFACE-RELATED SHELL THEORIES FOR THE NUMERICAL SIMULATION OF CONTACT PROBLEMS

RAINER SCHLEBUSCH
JAN MATHEAS
BERND W. ZASTRAU

Technische Universität Dresden, Dresden, Germany
Rainer.Schlebusch@mailbox.tu-dresden.de

This paper deals with a surface-related shell theory and its conversion into the finite element method for the investigation of composites and contact problems. In particular, composites made of a textile reinforced concrete are examined for the strengthening of existing shell structures. The interaction between the existing structure and the strengthening layer is considered as a contact problem involving adhesion.

Key words: shell theory, enhanced assumed strain method, contact problems

1. Introduction

For the design of textile reinforcement for the structural strengthening and restoration in static and dynamic applications suitable mechanical models need to be established. Basic features of the textile reinforced concrete can be found in Curbach (1998). As a possible application, the strengthening of a cylindrical tank, cp. Fig. 1, is considered. Reasons for the modification of the existing structural member could be the storing of a substance with a higher density or the increase of the filling height. If the load carrying capacity of the existing structure is not sufficient for the higher loading, an additional layer added to the outer surface might be the best way to improve the tank. Since, generally, the strengthening layer is thin, its mechanical description is favorably based on a shell theory. The present contribution to the development of a new composite material, textile reinforced concrete, is focused on the derivation of a suitable material description and shell theory. With respect

to the framework of application, the advantage is taken of the free, by principle, choice of the reference surface position by attaching the reference surface to one of the outer surfaces. The shell theory using an outer surface as the reference surface, which is therefore called the surface-related shell theory, is a natural approach for several reasons. Hereby the interface behavior is modelled as a contact problem which can take adhesion into account. The idea of surface-related shell theories was already pursued by one of the authors many years ago, cp. Rothert and Zastrau (1981), Zastrau (1983). Unlike in the standard shell theories, which refer to the middle surface of the shell, the models introduced here offer among others the following advantages:

- Contact problems can be considered without the usual difficulty of mapping the middle surface data onto the outer shell surface.
- The discretization of the contact surface and therewith the complete discretization may remain unchanged, in contrast to the classical approach. In an optimization of e.g. the utilization of a material, only the elements of those matrices which belong to elements coordinate to the surface, have to be changed iteratively.
- Discontinuities of the stress field, caused e.g. by concentrated loads occurring on the surface, which is peculiar to contact problems, can be directly determined where they occur.
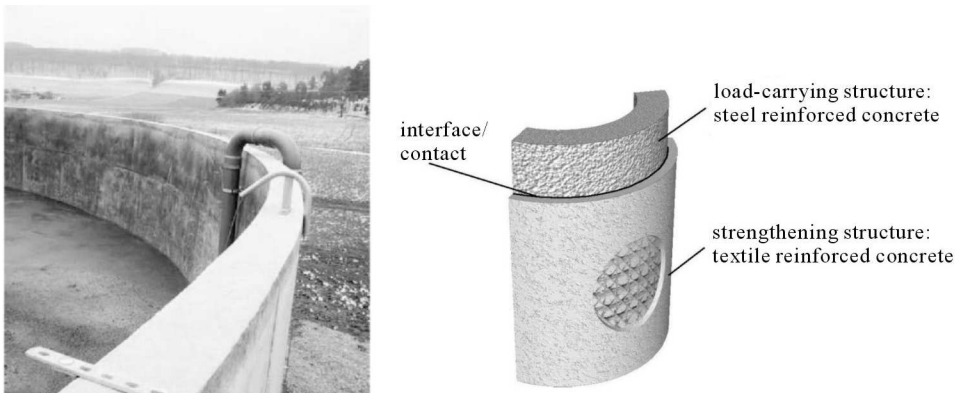- Easier detection of compound failure and delamination becomes possible.

Fig. 1. Picture of an existing structural member and the model of a cylindrical tank with a strengthening structure made of the textile reinforced concrete

In this context the paper by Zastrau *et al.* (2000) is also referred to, where a very general series expansion in the thickness-direction is proposed. If an

insufficient or a wrong set of terms for the series expansion is used, this so called Naghdi-model does not permit the usage of a three-dimensional, in general, constitutive relation without manipulating the constitutive relation itself. The application of the degeneration concept alone does not permit the usage of a three-dimensional constitutive relation, if for the semidiscretization of the displacements a linear series expansion in the thickness-direction is used. But in combination with the enhanced assumed strain (EAS) method its application becomes possible. This combination could be understood as a shell theory which comprises the minimal number of kinematic equations necessary to operate with a three-dimensional constitutive relation, cp. Bischoff (1999).

2.   Continuum mechanical considerations

The starting-point for the mechanical description of a strengthening structure is the Boltzmann continuum in Lagrangian representation, cp. Eringen (1989). Within the context of this paper, the description of the material behavior is restricted to isothermal and reversible processes. From this, the number of unknown fields is reduced to three: the displacement field U, the Green-Lagrange strain tensor $\mathbf{E}$ and the second Piola-Kirchhoff stress tensor $\mathbf{S}$, where these fields are not independent from each other. They are related to each other by:

— kinematic field equation

$$\mathbf{E} - \frac{1}{2}(\mathbf{F}^{\top} \cdot \mathbf{F} - \mathbf{G}) = \mathbf{E} - \mathbf{E}^{u} = \mathbf{0} \qquad \text{in} \quad \mathcal{B} \tag{2.1}$$

— constitutive relation

$$\mathbf{S} = \rho_0 \frac{\partial f}{\partial \mathbf{E}} = \mathcal{C} : \mathbf{E} \qquad \text{with} \qquad \mathcal{C} = \lambda \mathbf{G} \otimes \mathbf{G} + 2\mu \mathcal{I} \quad \text{in} \quad \mathcal{B} \tag{2.2}$$

— equilibrium equation

$$\mathrm{Div}\,(\mathbf{F} \cdot \mathbf{S}) + \rho_0 \boldsymbol{f} = \rho_0 \ddot{U} = \mathbf{0} \qquad \text{in} \quad \mathcal{B} \tag{2.3}$$

Herein $\mathcal{B}$ is the body in the reference configuration, $\mathbf{F} = \mathrm{Grad}\,\boldsymbol{x}$ – the deformation gradient, $\mathbf{G}$ – the metric tensor of the reference configuration, $\mathbf{E}^{u} = (\mathbf{F}^{\top} \cdot \mathbf{F} - \mathbf{G})/2$ – the displacement compatible Green-Lagrange strain tensor, f – the Helmholtz free energy, ρ_0 – the density in the reference configuration, $\mathcal{C}$ – the forth order elasticity tensor of the St. Venant-Kirchhoff

material, $\mathcal{I} = \mathbf{G} \boxtimes \mathbf{G}$ – the forth order identity tensor, and $\boldsymbol{f}$ – the body force per unit mass. In the definition of the identity tensor $\boxtimes$ symbolizes the squared tensor product, cp. Halmos (1948), del Piero (1979), defined by $\mathbf{A} \boxtimes \mathbf{B} : \mathbf{C} := \mathbf{A} \cdot \mathbf{C} \cdot \mathbf{B}^{\top}$. Additionally:

— dynamic boundary condition

$$\mathbf{F} \cdot \mathbf{S} \cdot \boldsymbol{N} = \bar{\boldsymbol{t}}_0 \qquad \text{on} \quad \partial_\sigma \mathcal{B} \tag{2.4}$$

— geometric boundary condition

$$\boldsymbol{U} - \overline{\boldsymbol{U}} = \boldsymbol{0} \qquad \text{on} \quad \partial_u \mathcal{B} \tag{2.5}$$

are stated to characterize the complete boundary-value problem. In (2.4) $\partial_\sigma \mathcal{B}$ is the part of the surface of the body in the reference configuration where the surface force per unit area of the boundary $\bar{\boldsymbol{t}}_0$ is prescribed, and in (2.5) $\partial_u \mathcal{B}$ is the part of the boundary of the body in the reference configuration where the displacements $\overline{\boldsymbol{U}}$ are prescribed. The superposed bar indicates prescribed quantities. In addition, $\boldsymbol{N}$ is the outer normal vector to the surface of the body in the reference configuration.

The weak form of the equilibrium equation leads to the principle of virtual displacements, which is the foundation for pure displacement finite elements. If the kinematic field equation (2.1) and the geometric boundary condition (2.5) are not eliminated but introduced into the principle of the minimum of potential energy by Lagrangian multipliers $\mathbf{S}$ and $\boldsymbol{t}_0$, the augmented Hu-Washizu functional is obtained. The demand for a minimum of the total energy in the principle of the minimum of the potential energy changes to a stationarity condition in the Hu-Washizu functional. It describes the following saddle point problem

$$\Pi(\mathbf{E}, \boldsymbol{U}, \mathbf{S}, \boldsymbol{t}_0) = \int_{\mathcal{B}} \rho_0 f \, dV + \int_{\mathcal{B}} \mathbf{S} : (\mathbf{E}^u - \mathbf{E}) \, dV - \int_{\mathcal{B}} \rho_0 \boldsymbol{f} \cdot \boldsymbol{U} \, dV$$

$$- \int_{\partial_\sigma \mathcal{B}} \bar{\boldsymbol{t}}_0 \cdot \boldsymbol{U} \, dA - \int_{\partial_u \mathcal{B}} \boldsymbol{t}_0 \cdot (\overline{\boldsymbol{U}} - \boldsymbol{U}) \, dA = \text{stat} \tag{2.6}$$

To simplify the four field functional (2.6) and to avoid an explicit interpolation for the stress field $\mathbf{S}$ the second term on the right-hand side is forced to vanish. This procedure characterizes the above mentioned EAS method which was first presented in the context of a variational formulation of continuum problems by Simo and Rifai (1990), and demands that the additional

strain tensor is orthogonal to the stress tensor. This results in the fact that the orthogonality condition

$$\int_{\mathcal{B}} \mathbf{S} : (\mathbf{E} - \mathbf{E}^u) \, dV = \int_{\mathcal{B}} \mathbf{S} : \widetilde{\mathbf{E}} \, dV = 0 \qquad \text{with} \qquad \widetilde{\mathbf{E}} = \mathbf{E} - \mathbf{E}^u \qquad (2.7)$$

in the discretized form must be fulfilled. The additional strain tensor $\widetilde{\mathbf{E}}$ enriches additively the displacement compatible strain tensor $\mathbf{E}^u$ to avoid locking phenomena in the shell theory and in the finite element formulation, respectively. This aspect will be discussed later on in conjunction with the formulation of the shell theory. The discretized additional strain tensor $\widetilde{\mathbf{E}}$ has to be linear independent of the displacement compatible strain tensor $\mathbf{E}^u$ to avoid singular stiffness matrices, see for details cp. Simo and Rifai (1990). In contrast to the hybrid stress concept, the EAS concept preserves the basic features of pure displacement finite elements, because the resulting additional strain parameters need not be compatible across the element boundary. They can be eliminated on the element level by condensation. The fulfillment of the orthogonality condition reduces four field Hu-Washizu functional (2.6) to a modified three field functional, which is the underlying principle for the surface-related shell theory and the finite element formulation

$$\Pi(\widetilde{\mathbf{E}}, \boldsymbol{U}, \boldsymbol{t}_0) = \int_{\mathcal{B}} \rho_0 f \, dV - \int_{\mathcal{B}} \rho_0 \boldsymbol{f} \cdot \boldsymbol{U} \, dV - \int_{\partial_\sigma \mathcal{B}} \overline{\boldsymbol{t}}_0 \cdot \boldsymbol{U} \, dA - \int_{\partial_u \mathcal{B}} \boldsymbol{t}_0 \cdot (\overline{\boldsymbol{U}} - \boldsymbol{U}) \, dA = \text{stat}$$

$$(2.8)$$

3. Surface-related shell theory

Since every shell theory is an approximation of the three dimensional continuum theory, basic assumptions have to be made, cp. Naghdi (1963), Başar and Krätzig (1985). The most serious assumption is related to the kinematics. Before the chosen kinematics is discussed in detail, the differential geometry of the shell continuum has to be described, cp. Fig. 2.

To reach this, a general curvilinear, convected coordinate system Θ^1, Θ^2 and Θ^3 is introduced in the shell continuum. With the aid of this parametrization, every point in the shell continuum is uniquely identified by the position vector $\boldsymbol{X}$. With the position vector $\boldsymbol{X}$ one obtains the base vectors $\boldsymbol{G}_i$ and
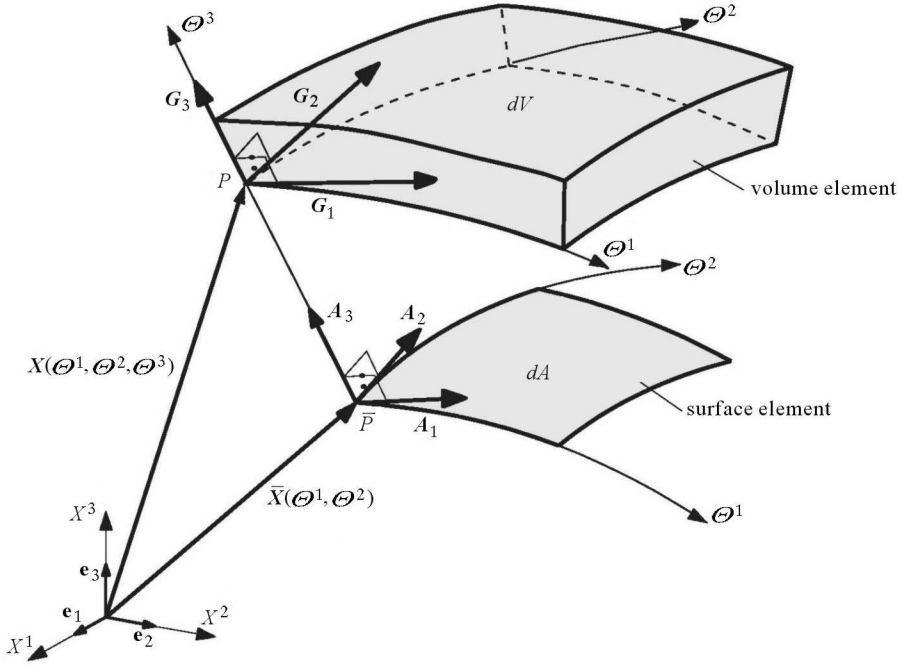
Fig. 2. Differential geometry of the shell

$\boldsymbol{G}^i$ as well as the Riemann metric tensor $\mathbf{G}$ of the shell space in the reference configuration as

$$\boldsymbol{G}_i = \boldsymbol{X}_{,i}$$

$$\mathbf{G} = \boldsymbol{G}_i \cdot \boldsymbol{G}_j \boldsymbol{G}^i \otimes \boldsymbol{G}^j = G_{ij}\boldsymbol{G}^i \otimes \boldsymbol{G}^j = \delta_i^j \boldsymbol{G}_j \otimes \boldsymbol{G}^i = \boldsymbol{G}_i \otimes \boldsymbol{G}^i$$

(3.1)

where δ_i^j is the Kronecker symbol and the comma is the partial derivation with respect to the convective coordinate Θ^i. With

$$\boldsymbol{G}_i \cdot \boldsymbol{G}^j = \delta_i^j \qquad G = \det(G_{ij}) \qquad dV = \sqrt{G}d\Theta^1 d\Theta^2 d\Theta^3 \qquad (3.2)$$

the contravariant base vectors and the volume element of the undeformed shell space are also introduced. Additionally, a space tangent to the shell reference surface is required. Analogous to (3.1) and (3.2) this leads to

$$\boldsymbol{A}_\alpha = \overline{\boldsymbol{X}}_{,\alpha}$$

$$\mathbf{A} = \boldsymbol{A}_\alpha \cdot \boldsymbol{A}_\beta \boldsymbol{A}^\alpha \otimes \boldsymbol{A}^\beta = A_{\alpha\beta}\boldsymbol{A}^\alpha \otimes \boldsymbol{A}^\beta = \delta_\alpha^\beta \boldsymbol{A}_\beta \otimes \boldsymbol{A}^\alpha = \boldsymbol{A}_\alpha \otimes \boldsymbol{A}^\alpha$$

(3.3)

and

$$\boldsymbol{A}_\alpha \cdot \boldsymbol{A}^\beta = \delta_\alpha^\beta \qquad A = \det(A_{\alpha\beta}) \qquad dA = \sqrt{A}d\Theta^1 d\Theta^2 \qquad (3.4)$$

where $\overline{\boldsymbol{X}} = \boldsymbol{X}(\Theta^\alpha, 0)$ is the position vector of the reference surface, see Fig. 2. In order to make the decomposition of tensors with components perpendicular to the shell reference surface possible, a third vector is introduced as

$$\boldsymbol{A}_3 = \boldsymbol{X},_3\Big|_{\Theta^3=0} = \frac{\boldsymbol{A}_1 \times \boldsymbol{A}_2}{|\boldsymbol{A}_1 \times \boldsymbol{A}_2|} \qquad (3.5)$$

and is called the unit normal vector. Since normal coordinates are used for Θ^3, it has the following properties

$$\boldsymbol{A}_3 \cdot \boldsymbol{A}_\alpha = 0 \qquad \boldsymbol{A}_3 \cdot \boldsymbol{A}_3 = 1 \qquad \boldsymbol{A}_3 = \boldsymbol{A}^3 \qquad (3.6)$$

If the partial derivative of $\boldsymbol{X} = \overline{\boldsymbol{X}} + \Theta^3 \boldsymbol{A}_3$ is formed, the following relationship between the base vectors $\boldsymbol{G}_i$ in the shell space and the base vectors $\boldsymbol{A}_i$ located in the reference surface can be established

$$\boldsymbol{G}_i = \mathbf{Z} \cdot \boldsymbol{A}_i \qquad (3.7)$$

introducing the shell shifter tensor in the following way

$$\mathbf{Z} = \boldsymbol{G}_i \otimes \boldsymbol{A}^i = \mu_i^j \boldsymbol{A}_j \otimes \boldsymbol{A}^i \qquad (3.8)$$

Therewith holds also

$$\mu = \det \mathbf{Z} = \sqrt{\frac{G}{A}} = 1 - 2\Theta^3 H + (\Theta^3)^2 K \qquad (3.9)$$

and it follows

$$dV = \mu\sqrt{A}\, d\Theta^1 d\Theta^2 d\Theta^3 = \mu\, d\Theta^3 dA \qquad (3.10)$$

where $H = (\operatorname{tr}\mathbf{B})/2$ and $K = \operatorname{tr}\overset{+}{\mathbf{B}}$ are the mean curvature H and the Gaussian curvature K of the surface respectively calculated from the curvature tensor $\mathbf{B} = -\boldsymbol{A}_\alpha \cdot \boldsymbol{A}_{3,\beta}\, \boldsymbol{A}^\alpha \otimes \boldsymbol{A}^\beta$ and its adjoint tensor. The shell shifter tensor is a two point tensor, cp. Ericksen (1960), allowing to replace the base vectors $\boldsymbol{G}_i$ and $\boldsymbol{G}^i$ with the base vectors $\boldsymbol{A}_i$ and $\boldsymbol{A}^i$. The shifter tensor is used to define so-called surface-related tensors which are labelled with hats. Firstly, it is used to shift the Green-Lagrange strain tensor $\mathbf{E}$

$$\mathbf{E} = \mathbf{Z}^{-\top} \boxtimes \mathbf{Z}^{-\top} : \widehat{\mathbf{E}} = E_{ij}\boldsymbol{G}^i \otimes \boldsymbol{G}^j$$

$$\widehat{\mathbf{E}} = \mathbf{Z}^\top \boxtimes \mathbf{Z}^\top : \mathbf{E} = E_{ij}\boldsymbol{A}^i \otimes \boldsymbol{A}^j$$

and, secondly, to shift the second Piola-Kirchhoff stress tensor $\mathbf{S}$

$$\mathbf{S} = \quad \mathbf{Z} \boxtimes \mathbf{Z} \quad : \widehat{\mathbf{S}} = S^{ij} \boldsymbol{G}_i \otimes \boldsymbol{G}_j$$

$$\widehat{\mathbf{S}} = \mathbf{Z}^{-1} \boxtimes \mathbf{Z}^{-1} : \mathbf{S} = S^{ij} \boldsymbol{A}_i \otimes \boldsymbol{A}_j$$

The orthogonality condition can be transformed into the following notation

$$\int_{\mathcal{B}} \mathbf{S} : \widetilde{\mathbf{E}} \, dV = \int_{\mathcal{B}} (\mathbf{Z} \boxtimes \mathbf{Z} : \widehat{\mathbf{S}}) : (\mathbf{Z}^{-\top} \boxtimes \mathbf{Z}^{-\top} : \widehat{\widetilde{\mathbf{E}}}) \, dV =$$

$$= \int_{\mathcal{B}} \widehat{\mathbf{S}} : \widehat{\widetilde{\mathbf{E}}} \, dV = \int_{\mathcal{B}} S^{ij} \widetilde{E}_{ij} \, dV = 0$$

$$(3.11)$$

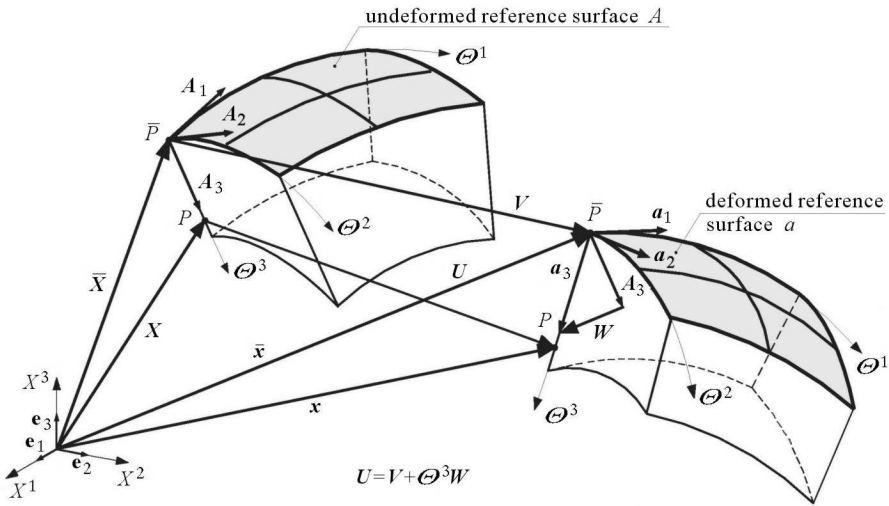which shows that the shifted quantities can also be used to evaluate the orthogonality condition.

Fig. 3. Undeformed and deformed part of the shell continuum and shell kinematics

Due to the displacement field $\boldsymbol{U}$, the shell continuum is deformed from the reference configuration into the actual configuration, see Fig. 3. This general deformation is restricted by a kinematical assumption. Within the scope of the presented shell formulation, it is assumed that the displacement field is a sum of two parts

$$\boldsymbol{U} = \boldsymbol{V} + \Theta^3 \boldsymbol{W} \tag{3.12}$$

first, the displacement field $\boldsymbol{V}$ of the reference surface and, second, a part in the direction of $\boldsymbol{W}$ being linear in the normal coordinate Θ^3. Here $\boldsymbol{W}$ is a

vector field describing the displacement of points along the normal vector. In general, the resulting vector a_3 is no longer perpendicular to the deformed reference surface a. Introducing the restricted displacement field (3.12) in the definition of the displacement compatible strain tensor, it can be determined as follows

$$\widehat{\mathsf{E}}^{\mathsf{u}} = [\alpha_{ij}^u + \Theta^3 \beta_{ij}^u + (\Theta^3)^2 \gamma_{ij}^u] \boldsymbol{A}^i \otimes \boldsymbol{A}^j = \boldsymbol{\alpha}^{\mathsf{u}} + \Theta^3 \boldsymbol{\beta}^{\mathsf{u}} + (\Theta^3)^2 \boldsymbol{\gamma}^{\mathsf{u}} \qquad (3.13)$$

with the sub-strain tensors

$$\boldsymbol{\alpha}^{\mathsf{u}} = \alpha_{ij}^u \boldsymbol{A}^i \otimes \boldsymbol{A}^j \qquad\qquad \boldsymbol{\beta}^{\mathsf{u}} = \beta_{ij}^u \boldsymbol{A}^i \otimes \boldsymbol{A}^j$$
$$\boldsymbol{\gamma}^{\mathsf{u}} = \gamma_{ij}^u \boldsymbol{A}^i \otimes \boldsymbol{A}^j \qquad\qquad (3.14)$$

and the sub-strain components

$$\alpha_{\alpha\beta}^u(\boldsymbol{V}, \boldsymbol{W}) = \frac{1}{2}(\boldsymbol{V},_\alpha \cdot \boldsymbol{A}_\beta + \boldsymbol{V},_\beta \cdot \boldsymbol{A}_\alpha + \boldsymbol{V},_\alpha \cdot \boldsymbol{V},_\beta)$$

$$\beta_{\alpha\beta}^u(\boldsymbol{V}, \boldsymbol{W}) = \frac{1}{2}[\boldsymbol{V},_\alpha \cdot (\boldsymbol{A}_{3,\beta} + \boldsymbol{W},_\beta) + \boldsymbol{V},_\beta \cdot (\boldsymbol{A}_{3,\alpha} + \boldsymbol{W},_\alpha) + \boldsymbol{W},_\alpha \cdot \boldsymbol{A}_\beta + \boldsymbol{W},_\beta \cdot \boldsymbol{A}_\alpha]$$

$$\gamma_{\alpha\beta}^u(\boldsymbol{V}, \boldsymbol{W}) = \frac{1}{2}(\boldsymbol{W},_\alpha \cdot \boldsymbol{A}_{3,\beta} + \boldsymbol{W},_\beta \cdot \boldsymbol{A}_{3,\alpha} + \boldsymbol{W},_\alpha \cdot \boldsymbol{W},_\beta)$$

$$\alpha_{\alpha3}^u(\boldsymbol{V}, \boldsymbol{W}) = \frac{1}{2}[\boldsymbol{V},_\alpha \cdot (\boldsymbol{A}_3 + \boldsymbol{W}) + \boldsymbol{W} \cdot \boldsymbol{A}_\alpha] \qquad (3.15)$$

$$\beta_{\alpha3}^u(\boldsymbol{V}, \boldsymbol{W}) = \frac{1}{2}[\boldsymbol{W} \cdot \boldsymbol{A}_{3,\alpha} + \boldsymbol{W},_\alpha \cdot (\boldsymbol{A}_3 + \boldsymbol{W})]$$

$$\gamma_{\alpha3}^u(\boldsymbol{V}, \boldsymbol{W}) = 0 \quad \alpha_{33}^u(\boldsymbol{V}, \boldsymbol{W}) = \frac{1}{2}\boldsymbol{W} \cdot (2\boldsymbol{A}_3 + \boldsymbol{W})$$

$$\beta_{33}^u(\boldsymbol{V}, \boldsymbol{W}) = 0 \quad \gamma_{33}^u(\boldsymbol{V}, \boldsymbol{W}) = 0$$

The disadvantage of the used 6-parameter shell kinematics is that it suffers from the so-called Poisson thickness locking, which will be shortly discussed. To explain the Poisson thickness locking, a beam with a rectangular cross-section as shown in Fig. 4 is examined. The material of the beam has a Poisson's ratio being unequal to zero. Due to pure bending a linear normal stress distribution over the beam thickness is obtained, for instance tension above the neutral axis and compression below. This results in transverse contraction in the upper half and transverse extension in the bottom half of the cross-section. According to the stress distribution the transverse normal strain is linearly distributed as well, while the overall thickness of the beam or of the shell, respectively, will
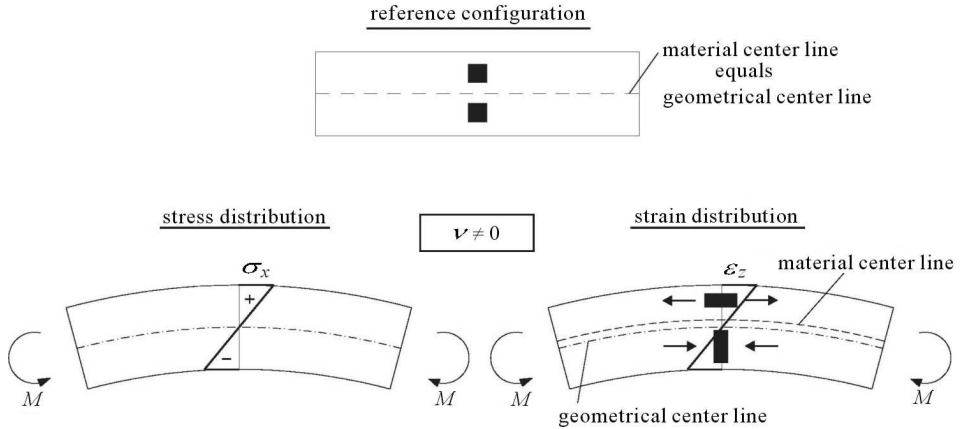
Fig. 4. Description of the origin of the Poisson thickness locking

remain unchanged. The material center line, that is the line of material points which are in the undeformed state located on the geometrical center line, moves up and is no longer located on the geometrical center line. Due to the chosen kinematics (3.12) such a linear distribution of the normal strain can not be represented. The corresponding transverse strain component β_{33}^u, cp. last Eq. (3.15), is equal to zero. This causes a constraint which prevents the material center line from motion and produces artificial transverse normal stresses. These so-called parasitical stresses contribute to the internal energy and finally to an increase in the stiffness of the pure displacement finite element. This means that, in bending dominated cases, a relative error of the order of ν^2 occurs, even in linear analysis, cp. Büchter (1992), Bischoff (1999). It is obviously not adequate to approximate the deformation of a shell with unchanging thickness by the kinematics (3.12), because this leads to $\beta_{33} = 0$. To avoid this locking effect an enhancement of the Green-Lagrange strain tensor is made using the EAS method. The enhancement is the following

$$\widetilde{E}_{33} = \Big(\frac{H}{2} - \Theta^3\Big)\widetilde{\beta}_{33} \tag{3.16}$$

Accordingly, the enrichment of the strain field has only one component. It is important to note that this single component is sufficient to avoid the Poisson thickness locking, because it introduces the missing, in Θ^3 linearly varying, expression into the transverse normal strain. Due to the special position of the reference surface, a shift about the half thickness $H/2$ of the shell is necessary to ensure that the additional strain is zero, if it is calculated in the location of

the middle surface. Before the additional strain $\widetilde{E}_{33}$ can be determined, some additional notations and definitions have to be introduced.

The integration of the shifted second Piola-Kirchhoff stress tensor $\widehat{\mathbf{S}}$ over the thickness H of the shell defines the stress resultant tensors of the shell theory

$$\mathbf{n} = n^{ij}\boldsymbol{A}_i \otimes \boldsymbol{A}_j = \int_0^H \widehat{\mathbf{S}}(\Theta^3)^0 \det \mathbf{Z}\, d\Theta^3 = \int_0^H S^{ij}(\Theta^3)^0 \mu\, d\Theta^3 \boldsymbol{A}_i \otimes \boldsymbol{A}_j$$

$$\mathbf{m} = m^{ij}\boldsymbol{A}_i \otimes \boldsymbol{A}_j = \int_0^H \widehat{\mathbf{S}}(\Theta^3)^1 \det \mathbf{Z}\, d\Theta^3 = \int_0^H S^{ij}(\Theta^3)^1 \mu\, d\Theta^3 \boldsymbol{A}_i \otimes \boldsymbol{A}_j \quad (3.17)$$

$$\mathbf{s} = s^{ij}\boldsymbol{A}_i \otimes \boldsymbol{A}_j = \int_0^H \widehat{\mathbf{S}}(\Theta^3)^2 \det \mathbf{Z}\, d\Theta^3 = \int_0^H S^{ij}(\Theta^3)^2 \mu\, d\Theta^3 \boldsymbol{A}_i \otimes \boldsymbol{A}_j$$

It should be mentioned that it is characteristic to the presented surface-related shell theory to integrate from zero to H corresponding to the particular position of the reference surface. The stress resultants are called the membrane ($\mathbf{n}$), the moment ($\mathbf{m}$) and the bi-moment ($\mathbf{s}$) stress resultant tensor, respectively.

If the constitutive relation (2.2) is also shifted to the reference surface and introduced into the formerly stated definitions of stress resultants $(3.17)_1$ to $(3.17)_3$, the pre-integration over the shell thickness is accomplished and the decomposition into sub-strain tensors (3.13) is used, the constitutive relation can be expressed by the components of the stress resultants and of the sub-strain tensors

$$\begin{bmatrix} n^{ij} \\ m^{ij} \\ s^{ij} \end{bmatrix} = \begin{bmatrix} D_0^{ijkl} & D_1^{ijkl} & D_2^{ijkl} \\ D_1^{ijkl} & D_2^{ijkl} & D_3^{ijkl} \\ D_2^{ijkl} & D_3^{ijkl} & D_4^{ijkl} \end{bmatrix} \begin{bmatrix} \alpha_{kl} \\ \beta_{kl} \\ \gamma_{kl} \end{bmatrix} \quad (3.18)$$

Herein, the matrix elements D_0^{ijkl} to D_4^{ijkl} are defined by the following integrals

$$D_K^{ijkl} = \int_0^H (\Theta^3)^K C^{ijkl} \mu\, d\Theta^3 \qquad \text{with} \quad K \in \{0, 1, 2, 3, 4\} \quad (3.19)$$

For an efficient determination of the integral the determinant of the shell shifter tensor μ is often set equal to one, and the last row and column are also often neglected in the constitutive matrix (3.18).

With the aid of these definitions, it is now possible to determine the value of the additional strain parameter $\widetilde{\beta}_{33}$ by exploiting thr orthogonality condition (3.11)

$$\int\limits_V S^{33}\widetilde{E}_{33}\,dV = 0 \tag{3.20}$$

Furthermore this yields to

$$m^{33} - n^{33}\frac{H}{2} = 0 \tag{3.21}$$

The herein enclosed coupling of the membrane (n^{33}) and moment (m^{33}) stress resultant tensor is characteristic to surface-related shell theories. If the reference surface is identical with the middle surface, the evaluation of orthogonality condition (3.20) leads to $m^{33} = 0$, which is likewise equivalent to the statement that in the case of pure bending no transverse normal stresses occur. Consequently, the Poisson thickness locking is avoided with the aid of the EAS method. As desired no parasitical transverse normal stresses occur in the case of pure bending. With equation (3.21) the value of the additional strain parameter $\widetilde{\beta}_{33}$ can finally be determined from

$$\widetilde{\beta}_{33} = \frac{[D_1^{33kl}, D_2^{33kl}, D_3^{33kl}] - \frac{H}{2}[D_0^{33kl}, D_1^{33kl}, D_2^{33kl}]}{-D_0^{3333}\frac{H^2}{4} + D_1^{3333}H - D_2^{3333}}\begin{bmatrix} \alpha_{kl}^u \\ \beta_{kl}^u \\ \gamma_{kl}^u \end{bmatrix} \tag{3.22}$$

The value of $\widetilde{\beta}_{33}$ depends on the elements of the constitutive matrix (3.18) and the displacement compatible sub strains (3.15). Interpreting the additional strain parameter as a kinematical variable one can speak of a 7-parameter shell theory. This is valid, because the strain parameter can be determined in any point of the reference surface. However, it should be mentioned that this seventh parameter can be eliminated on the element level. This results again in a 6-parameter shell theory. Hence, an expansion of the element stiffness matrix and the system stiffness matrix is prevented by the aforementioned elimination.

4. Contact mechanics

For the investigation of the behavior of the textile reinforced concrete strengthening of an existing load-carrying structure, the contact mechanics,

which is described extensively in Laursen and Simo (1993), Wriggers (1995), is utilized. The aim is to build the tangential stiffness matrix for the normal and tangential contact with the help of contact segments which are placed on the outer surface of the shell element. These segments can be easily used with a body situated in contact that is discretized by volume elements. The difficulty in the middle surface related shell elements is the estimation of the stiffness for tangential and normal displacement degrees of freedom determined by the segments, because they directly effect the stiffness affiliated to the rotational degrees of freedom of the shell element. Using shell theories with higher order kinematics, this mapping from surface data on the middle surface is connected with considerable effort. Furthermore, it is necessary to know the geometry of the shell element connected with the contact segment. A combination of the contact segment and the shell element becomes unavoidable. Using surface-related shell theories, the assignment of the segments can be performed in the same manner like using volume elements, because only the stiffness corresponding to the three displacements has to be calculated. The coordinate systems of the contact segment as well as of the shell element are both situated in the contact area.

The principle of the virtual work can be utilized to derive the tangential stiffness matrix of the shell element because of the normal and tangential contact conditions in the case of sticking contact partners. If the tangential contact stress exceeds a static limit, which can either be dependent on the contact normal pressure p in the form $\tau_{\mathrm{max}} = \mu p$ with μ as the coefficient of friction or be independent with $\tau_{\mathrm{max}} = \tau_{\mathrm{stick}}$, then the shear stress

$$\boldsymbol{\tau}(g_N, \boldsymbol{g}_T) = -\frac{\boldsymbol{g}_T}{|\boldsymbol{g}_T|}[\mu p(g_N) + k(\boldsymbol{g}_T)] \qquad (4.1)$$

is used in the case of slipping. It depends on the gap function g_N and the tangential relative displacements represented by the slip vector $\boldsymbol{g}_T$. The first part in (4.1) states Coulomb's friction law. The resulting stiffness $k(\boldsymbol{g}_T)$ can be regarded as the tangential compound stiffness, e.g. adhesion within the contact area. This offers the possibility to describe compound problems within the scope of contact mechanics.

5. Locking phenomena

Among others, the kinematical restriction (3.12) and the interpolation of the degrees of freedom, which is realized by Lagrangian polynomials, are

the source of several locking phenomena, cp. Bischoff (1999), Bischoff and Ramm (1997). In particular, the following phenomena should be named in this context:

- Poisson thickness locking
- membrane locking
- volume locking
- curvature thickness locking
- shear locking

Hence, arrangements have to be made to reduce or avoid these locking effects, because all the artificial stiffening effects cause a significant deviation from the continuum mechanical solution. In this context the appropriate concepts shall only be stated. For more details the reader is referred to the cited literature. As described before, in connection with the formulation of the shell theory the EAS method is used to prevent the Poisson thickness locking. The described specialization is in close relation to Büchter and Ramm (1992), Büchter *et al.* (1994). Furthermore, the EAS method is used to prevent or reduce the membrane and volume locking. An effective concept against the curvature thickness locking is the ANS method having a variational justification, cp. Simo and Hughes (1986), whereas the discrete shear gap (DSG) method, cp. Bletzinger *et al.* (1998), shows high efficiency to avoid the shear locking. With a combination of the aforementioned concepts a very efficient finite volume shell element has been developed. The applicability of the presented finite element is demonstrated in the following numerical examples.

6.   Numerical examples

The first example is a square plate with build-in edges and a central point load. The geometry and material data are given in Fig. 5. The geometry, the material data and the value of the central point load are selected in such a way that the central deflection of the plate is 0.01 m, if the Kirchhoff plate theory is used to calculate the deflection. Making use of the symmetry, only one quarter of the plate is dicretized with 8-node shell elements. The number of elements per edge is varied, thus the fineness of the discretization varies as well. Because this example represents a bending dominated problem, the Poisson thickness locking and shear locking are expected even in the considered linear analysis. The results of this example are shown in Fig. 6. The diagram shows that the

pure displacement element does not reach the exact solution, even if more than ten elements per edge are used. That is, a too coarse discretization results in entirely useless results.
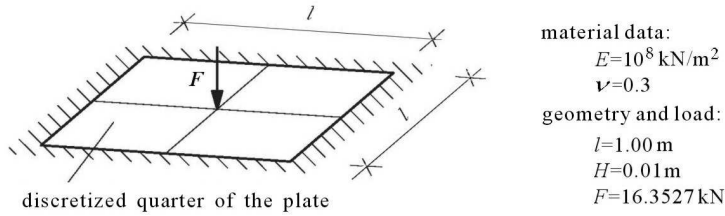

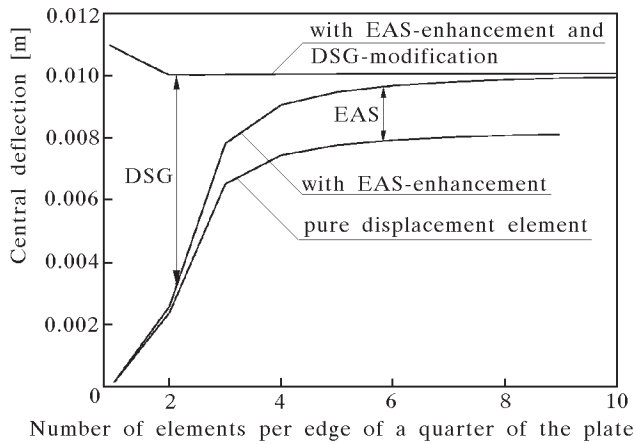Fig. 5. Square plate with build-in edges and a central point load

Fig. 6. Central deflection of the plate as a function of the number of elements per edge

However, the results can obviously be improved, if the EAS method and the DSG method come into operation. A discretization with 2×2 elements is fine enough to reach very good results in comparison with the analytical solution. Even if only one element is used and the relative error of approximately 10% can be accepted, the element leads to good results in the framework of application. Additionally performed numerical tests show in this example that the developed shell element is also insensitive to distorted discretizations. That is, the element gives reliable results in bending dominated plate problems even in coarse as well as in distorted discretizations.

For a further numerical test a circular plate with a circular hole as shown in Fig. 7 is analyzed, which was also examined by Başar and Ding (1990). The
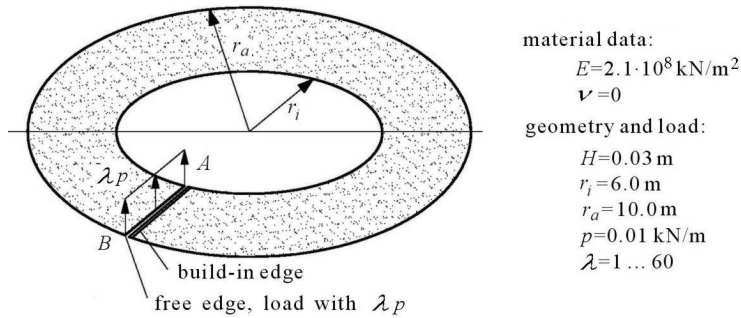
Fig. 7. Perspective view of a circular plate with a circular hole at the center
according to Başar and Ding (1990)

material data, the geometry and the load are given in Fig. 7. The circular plate
is coarsely discretized by one element in the radial direction and 16 elements in
the circumferential direction. The vertical deflection of the points A and B is
examined. The calculated results are nearly equal to those given in literature,
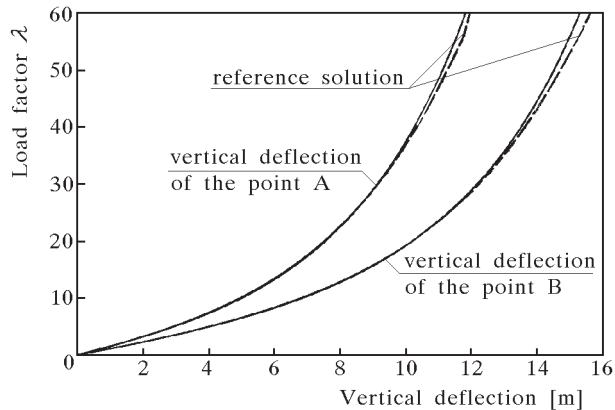Büchter (1992), Klinkel (2000).

Fig. 8. Diagram of the vertical deflection of the points A and B

The maximum relative deviation is less than 2%. The vertical deflections
of the points A and B are depicted in Fig. 8 as a function of the load factor λ.
The reference solution is taken from Büchter (1992), and is calculated with a
discretization of 30×6 4-node shell elements.

Figure 9 shows an unscaled drawing of the deformed configuration of the
circular plate under the maximum load. The gray shading illustrates the ab-
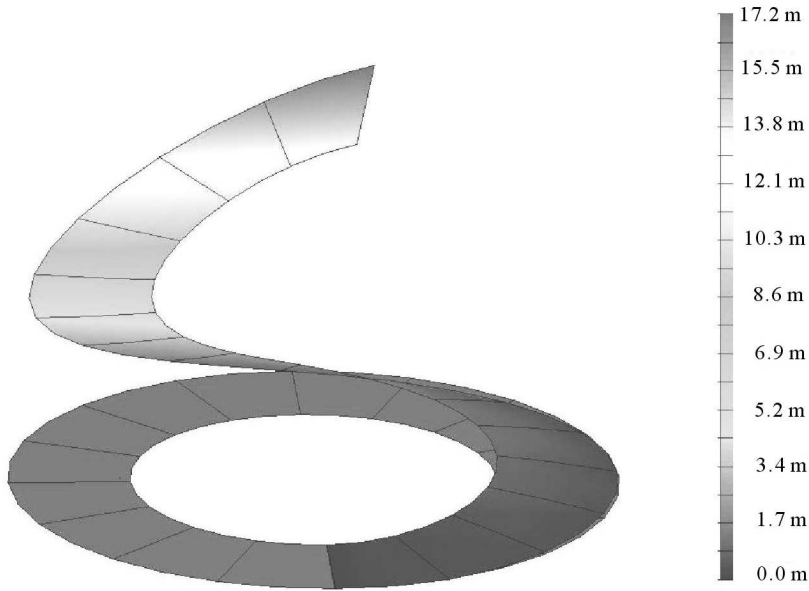solute value of the displacement.

Fig. 9. Deformed circular plate under maximum load

The last example should show the application of the contact mechanics. We choose a square plate, $7.20 \times 7.20 \times 0.20\,\mathrm{m}^3$, with simply supported edges and a central point load. The plate is made of St. Venant-Kirchhoff material with Young's modulus $E = 2.5 \cdot 10^7\,\mathrm{kN/m}^2$ and Poisson's ratio $\nu = 0.2$. The plate is strengthened by a symmetrically applied textile reinforced concrete ply, $6.30 \times 6.30 \times 0.02\,\mathrm{m}^3$, that is pressed against the plate by a contact pressure of $0.1\,\mathrm{kN/m}^2$ to establish the contact.
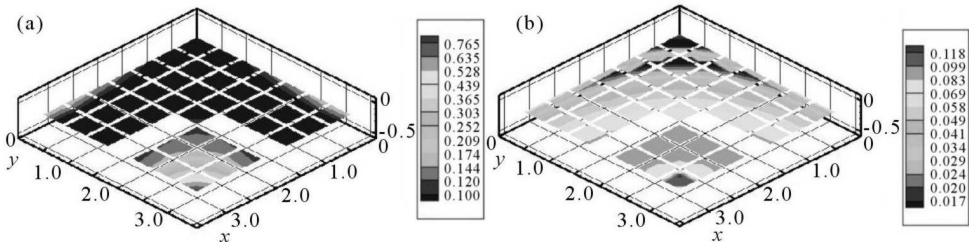

Fig. 10. Contact area and contact pressure (a) and contact shear stress distribution (b) $F = 3.75\,\mathrm{kN}$

For the maximum shear stress the friction coefficient $\mu_0 = \mu = 0.15$ is assumed, cp. (4.1). Young's modulus of the strengthening is $E = 2.0 \cdot 10^7\,\mathrm{kN/m}^2$
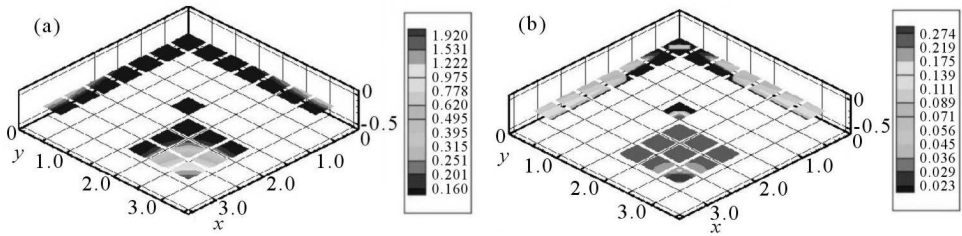
Fig. 11. Contact area and contact pressure (a) and contact shear stress
distribution (b) $F = 10.0\,\mathrm{kN}$

and Poisson's ratio is $\nu = 0.2$. Making use of the symmetry, only one quarter of the plate is dicretized with 4-node shell elements. In the first step, the central point load of $F = 3.75\,\mathrm{kN}$ was applied, see the results in Fig. 10, and in the second step to central point load F was $10\,\mathrm{kN}$, see the results in Fig. 11. The white areas in the contact domain represent delaminated regions of the strengthening layer. The size of the delaminated regions grows extensively with an increase in the load F. Only a quadratic region in the plate center and a strip near the edge stay in contact.

7. Conclusions

The formulation of surface-related shell theories allows an efficient simulation of the compound behavior of textile reinforced concrete layers for the strengthening of shell structures. Due to the particular position of the reference surface, the well established concepts against the locking phenomena are extended and implemented, which leads to a reliable surface-related finite volume shell element. With the aid of several different nonlinear examples, the efficiency of the developed shell and contact formulation is demonstrated.

References

1. Başar Y., Ding Y., 1990, Finite-rotation shell elements for analysis of finite-rotation shell problems, *Second World Congress on Computational Mechanics*, 785-788

2. Başar Y., Krätzig W.B., 1985, *Mechanik der Flächentragwerke*, Friedrich Vieweg & Sohn Verlag mbH, Braunschweig

3. Bischoff M., 1999, Theorie und Numerik einer dreidimensionalen Schalenformulierung, Ph.D. Thesis, Universität Stuttgart, Stuttgart

4. Bischoff M., Ramm E., 1997, Shear deformable shell elements for large strains and rotations, *International Journal for Numerical Methods in Engineering*, **40**, 4427-4449

5. Bletzinger K.U., Bischoff M., Ramm E., 1998, A unified approach for shear-locking-free triangular and rectangular shell finite elements, *Computational Mechanics, New Trends and Applications, CD-Rom Proceedings of the Fourth World Congress on Computational Mechanics*, 1-22

6. Büchter N., 1992, Zusammenführung von Degenerationskonzept und Schalentheorie bei endlichen Rotationen, Ph.D. Thesis, Universität Stuttgart, Stuttgart

7. Büchter N., Ramm E., 1992, 3D-extension of nonlinear shell equation based on the enhanced assumed strain concept, *First European Conference on Numerical Methods in Engineering*, 39-59

8. Büchter N., Ramm E., Roehl D., 1994, Three-dimensional extension of nonlinear shell formulation based on the enhanced assumed strain concept, *International Journal for Numerical Methods in Engineering*, **37**, 2551-2568

9. Curbach M., 1998, *Sachstandbericht zum Einsatz von Textilien im Massivbau, DBV 203*, Deutscher Beton-Verein E. V.

10. Del Piero G., 1979, Some properties of the set of fourth-order tensors, with application to elasticity, *Journal of Elasticity*, **9**, 3, 245-261

11. Ericksen J.L., 1960, Tensor fields, *Handbuch der Physik III/1*, Springer-Verlag, 794-858

12. Eringen A.C., 1989, *Mechanics of Continua*, Robert E. Krieger Publishing Company, Malabar, Florida

13. Halmos P.R., 1948, *Finite Dimensional Vector Spaces*, Princeton Univ. Pr. [u.a.], Princeton, New York

14. Klinkel S., 2000, Theorie und Numerik eines Volumen-Schalen-Elementes bei finiten elastischen und plastischen Verzerrungen, Ph.D. Thesis, Universität Karlsruhe, Karlsruhe

15. Laursen T.A., Simo J.C., 1993, A continuum-based finite element formulation for the implicit solution of multibody, large deformation frictional contact problems, *International Journal for Numerical Methods in Engineering*, **36**, 3451-3485

16. Naghdi P.M., 1963, Foundations of elastic shell theory, *Progress in Solid Mechanic*, **4**, 1-90

17. Rothert H., Zastrau B., 1981, Herleitung und Anwendung einer kontaktproblemorientierten Schalentheorie, *Konstruktiver Ingenieurbau-Berichte (KIB)*, **61/39**, 76-84

18. Simo J.C., Hughes T.J.R., 1986, On the variational foundations of assumed strain methods, *Journal of Applied Mechanics*, **53**, 51-54

19. Simo J.C., Rifai M.S., 1990, A class of mixed assumed strain methods and the method of incompatible modes, *International Journal for Numerical Methods in Engineering*, **29**, 1595-1638

20. Wriggers P., 1995, Finite element algorithms for contact problems, *Archives of Computational Methods in Engineering*, **2**, 4, 1-49

21. Zastrau B., 1983, Ein Beitrag zur Modifikation der klassischen Schalentheorie für die unmittelbare Berechnung von Kontaktproblemen, *Zeitschrift für Angewandte Mathematik und Mechanik*, **63**, 224-225

22. Zastrau B., Schlebusch R., Matheas J., 2000, Surface-related shell theories for the treatment of composites and contact problems, *Proceedings of the Fourth Colloquium on Computation of Shells and Spatial Structures*, 76-84

Powierzchniowe teorie powłok w numerycznej symulacji problemu kontaktowego

Streszczenie

W pracy omówiono problem powierzchniowej teorii powłok i jej konwersji do metody elementów skończonych w kontekście badań kompozytów i zagadnienia kontaktowego. W szczególności zajęto się kompozytami osnową cementową wzmacnianą materiałem tekstylnym jako komponentem nośnych konstrukcji powłokowych. Uwagę skoncentrowano na oddziaływaniu, jakie zachodzi pomiędzy strukturą nośną i wzmacniającą w takich powłokach. Przedstawiono analizę tego oddziaływania jako zagadnienia kontaktowego z włączeniem zjawiska adhezji.